

Stretched spin strength in ^{26}Mg and ^{30}Si

J. A. Carr

Supercomputer Computations Research Institute, Florida State University, Tallahassee, Florida 32306

(Received 22 November 1993)

Calculations have been made to explore the effect of configuration mixing in a large basis on the fragmentation of “stretched” $M6$ strength in the sd -shell nuclei ^{26}Mg and ^{30}Si . This work extends a study made for $N = Z$ sd -shell nuclei to midshell $N \neq Z$ nuclei with the same Hamiltonian and basis restriction, one particle in the $1f_{7/2}$ orbit and unrestricted occupancy of the sd -shell orbits, used in that earlier work. It is found that configuration mixing in this large basis gives a very good description of the total isovector strength seen in ^{26}Mg but fails to give a detailed description of the experimental spectra. Results for fragmentation of the isoscalar response are less conclusive because of conflicts between data sets.

PACS number(s): 21.60.Cs, 21.10.Re, 27.30.+t, 23.20.Js

I. INTRODUCTION

The $1\hbar\omega$ stretched spin response observed with one-step inelastic scattering reactions is of particular interest because it provides a way to monitor the fragmentation of a *single* particle-hole configuration. This particle-hole configuration is called “stretched” to indicate that it couples the maximum possible hole and particle angular momenta, $j_h = \ell_h + \frac{1}{2}$ and $j_p = \ell_p + \frac{1}{2}$, in the valence shell and the shell lying immediately above it to the maximum total angular momentum $J = j_h + j_p$. This unique component of a state’s wave function is selectively excited in MJ transitions provided single-particle excitations with energies $\geq 3\hbar\omega$ can be neglected [1–4]; further, the scattering cross section can be expressed in terms of a single transition density for a variety of probes, simplifying the comparison between data and theory [2, 5]. These features are preserved even if the strength is fragmented by configuration mixing within a $(0+1)\hbar\omega$ model space [4]. The stretched states in the sd -shell nuclei discussed here are 6^- states produced by an $M6$ excitation of the $1f_{7/2}1d_{5/2}^{-1}$ configuration.

Historically, an overview of the experimental data [6] suggested there was only one isovector stretched state in a given nucleus and this state carried only a small fraction (usually no more than 1/3) of the expected strength in the many self-conjugate nuclei studied. Several investigators looked at different ways that this strength could be quenched by mixing with states far away in the spectrum so that the displaced strength could not be seen experimentally. Calculations indicated that non-nucleonic degrees of freedom such as the Δ made a negligible contribution to the reduction of observable stretched strength [7–9]. The stretched configuration can also mix with particle-hole excitations involving the core and high-lying shells, which would also be expected to reduce the observed $M6$ rate. Core-polarization calculations with realistic interactions produce about half of the needed strength reduction [10–15]; however, as emphasized in Ref. [3], the large difference in the quenching of isoscalar and isovector strength is not reproduced by this approach [13, 15].

An alternate mechanism for the reduction of the observed stretched spin strength is that this reduction is a result of fragmentation, where mixing with other $1\hbar\omega$ configurations causes the strength to be redistributed with only the largest fragments being easily observable [16–19]. Recent experiments performed with high resolution and good statistics have been able to identify weak states carrying additional stretched strength [20, 21], and calculations showed that fragmentation in a suitably large shell-model basis can explain many aspects of the reduction and redistribution, relative to single-particle estimates, of observed stretched spin strength in $N = Z$ sd -shell nuclei [19, 22]. The calculations of Ref. [19] were made in a basis that allowed one particle in the $1f_{7/2}$ orbit with some restrictions in the sd shell; the final results [22] had no restrictions in the sd shell. This subset of the $(0+1)\hbar\omega$ basis proved quite successful in explaining the strength distribution in midshell nuclei. In particular, the prediction [19] of an observable concentration of $M6$ strength about 3 MeV above the yrast $6^-, T = 1$ state in ^{28}Si was later confirmed by results of a (p, n) experiment [21].

It is the distribution of strength in the spectrum that contains information crucial to understanding the role of fragmentation on spin excitations, but often the weaker fragments cannot be seen experimentally. For example, the isoscalar strength is so heavily fragmented in $N = Z$ nuclei that only a few $T = 0$ states have ever been seen. The situation can be different in $N \neq Z$ nuclei because mixing between neutron and proton configurations leads to an interference between isoscalar and isovector amplitudes, sometimes enhancing our ability to observe states carrying isoscalar stretched strength.

Fairly detailed analyses have been done in ^{14}C by Kurath (based on a variation of the Millener-Kurath interaction from Ref. [16]) for comparison to pion scattering data in Ref. [23], and in ^{26}Mg by Amusa and Lawson (with the Hamiltonian and basis described in Ref. [17]) for comparison to proton scattering data in Ref. [24]. The former used a $(1p)^{-3}(2s1d)$ space and gave a good description of the three observed states, including the neutron-isoscalar-proton pattern (as one goes up in ex-

citation energy) of the isospin structure of the $T = 1$ states, although the strength is overestimated by a factor of about 2. The latter used a fairly restrictive basis, limiting active particles to the $(1d_{5/2}1s_{1/2})^{11}(1f_{7/2})$ space, and badly overestimated the strength in the lowest states while getting some features of the spectrum correct.

Other analyses of $N = Z + 2$ nuclei include that of Millener [25] applied to the data of Manley *et al.* [26] for ^{18}O and calculations in the $g_{9/2}f_{7/2}^{-3}$ basis for ^{54}Fe [27]; these results are qualitatively similar to the ones described above in that the observed stretched strength is overestimated by the theory. In addition, a calculation for ^{38}Ar by Brown in an *sdpf* basis allowing up to one-particle–three-hole (1p-3h) excitations has been compared to (p, n) data in Ref. [28]; here we see good agreement with the data although a detailed comparison to states with different T was not possible.

The only study done for the nuclei of interest here was performed for ^{26}Mg in a very limited basis [24]. We have already seen that extending this basis improves agreement between theory and experiment for midshell $N = Z$ nuclei [22], so it is of interest to extend that work to include the neighboring $N \neq Z$ nuclei of ^{26}Mg and ^{30}Si within the same $(sd)^{n-1}f_{7/2}$ basis truncation of the full $(0 + 1)\hbar\omega$ space. In the remainder of this paper, Sec. II presents a review of the methods employed in the calculation, Sec. III shows the results for ^{26}Mg and compares them to a wide variety of experimental data, predictions for the ^{30}Si $M6$ response appear in Sec. IV, and we close with a summary of our conclusions.

II. METHODS

An earlier paper [22] gives a detailed description of the methods used for this study. Here we give a short summary of the key elements necessary to place these results in the context of other work.

These calculations were performed in the $(sd)^{n-1}f_{7/2}$ basis, where $n = A - 16$, so there are no restrictions in the *sd* shell. The Hamiltonian consists of the Wildenthal effective interaction for the full *sd* shell [29] and the “best fit” Schiffer-True central spin-dependent interaction [30] for the interaction between the *sd* and *f* configurations. The latter is constructed from the second set of entries in Table XVI of Ref. [30] with $r_1 = 1.45$ fm and $r_2 = 2.0$ fm and is evaluated for harmonic-oscillator radial functions with $\nu = 0.293$, corresponding to a size parameter $b = 1.847$ fm, to be consistent with our previous work [19, 22] and that of Amusa and Lawson [17, 24]. The $f_{7/2}$ single-particle energy was held fixed at the value required [22] to give the correct excitation energy for the lowest 6^- , $T = 0$ state in ^{28}Si . There are no free parameters in these calculations.

We are interested in matrix elements that measure the $M6$ response seen in inelastic scattering ($T_z = 0$) or charge exchange ($T_z = \pm 1$) reactions. It is particularly convenient to use Raynal’s Z coefficient, which is defined by

$$Z_{T,T_z} = \langle \Psi_{6^-,T} \| A_{T,T_z}^6(f_{7/2}, d_{5/2}) \| \Psi_{\text{g.s.}} \rangle \quad (1)$$

(reduced in spin space only) where

$$A_{T,T_z}^{6,M}(j_f, j_i) = \left[a_{j_f m_f, t_z f}^\dagger a_{j_i m_i, t_z i} \right]_{T, T_z}^{6, M}. \quad (2)$$

In Eq. (2), a^\dagger creates a particle, a annihilates one, and the square brackets denote the Clebsch-Gordan coefficients and phase factors required [31] to couple these operators to total angular momentum 6 and isospin T . Note that $\Psi_{\text{g.s.}}$ has $J^\pi = 0^+$ and $T = 1$ so the isovector $A_{T=1}^6$ operator connects it to states with isospin $T \pm 1$ or T . The simplicity of the “stretched” states guarantees that the inelastic-scattering cross section is proportional to Z_T^2 for all probes considered.

As described in detail in Ref. [22], the Lanczos algorithm [32] is used to avoid performing a full diagonalization in the very large vector spaces considered here. In particular, we employ the “collective vector” method [33], which exploits a special feature [34] of the Lanczos method. Here one applies the operator $A_{T,T_z}^{6,6}$ to the model ground state and then forms a vector with good isospin from the result. (This last step was not necessary for the $N = Z$ nuclei considered earlier.) This collective vector contains all of the $M6$ strength for isospin transfer T to states with a given isospin, and can be used to measure Σ , a “sum rule” that gives the integral of Z_T^2 in our basis space. The collective vector is not an eigenstate of the Hamiltonian; instead it is used to initiate the Lanczos iteration, making it particularly easy to compute the $M6$ spectrum from eigenenergies and widths of the pseudoeigenstates formed after any arbitrary number of iterations.

It is important to emphasize that we iterate until a satisfactory level of convergence has been reached, but that we never obtain the *exact* model eigenstate of the Hamiltonian within our basis restriction. Because the *pseudoeigenstate* is not an eigenstate of the model H , it acquires a width reflecting the uncertainty in the actual energy where the $M6$ strength associated with that pseudoeigenstate is located. However, as Whitehead has shown [34], the strength distribution for the set of pseudoeigenvectors formed after N iterations gives a description of the $M6$ spectrum accurate to the $(2N - 1)$ th moment; that is, it is a good approximation to the excitation-energy distribution from the actual model result and contains the information we wish to compare to the measured $M6$ response.

As before, the calculated spectra shown in the figures are based on the magnitude of Z^2 for the individual pseudoeigenstates spread by a Gaussian with the calculated width or 100 keV, whichever is larger. A spectrum generated in this way shows the envelope of the $M6$ strength distribution and is proportional to the inelastic-scattering cross section at the peak of the angular distribution; however, one must keep in mind that the broad bumps represent a large number of small states with the given distribution. The artificial width of 100 keV for converged states helps make the spectrum resemble a real one and facilitates comparison to experimental data.

The “data points” are placed at a height corresponding to the top of a Gaussian of this same 100 keV width and an area equal to the measured strength. The reader should compare these data points to the extreme top of

the theoretical peak for converged states. We will also find it convenient to display some data with histogram bars. Provided the width of a rectangular bar is chosen to be 250 keV, we can compare the height of the bar to these “data points” and/or the area of the bar to the area under the Gaussian curve.

As in previous work in this truncated basis, we cannot do anything about the presence of spurious center-of-mass motion in these wave functions. There is no practical way to separate spurious motion in anything less than a full $1\hbar\omega$ calculation. We do measure the spuriousity of the states of interest by evaluating the diagonal matrix element of the center-of-mass Hamiltonian. The measured spuriousities are typically only a few percent for the states of interest.

All calculations were done with the VLADIMIR system of codes [35] adapted to UNIX and optimized for the Cray Y-MP computer at Florida State.

III. ^{26}Mg

The situation in ^{26}Mg is that the $d_{5/2}$ neutron level is filled but the $d_{5/2}$ proton level is not. Transfer reaction data [36] indicate that neutron and proton pickup reactions on ^{26}Mg each populate a single $\frac{5}{2}^+$ state, just as in the neighboring self-conjugate nuclei. Thus the neutron response might be expected to resemble the situation in ^{28}Si , where there is a strong yrast state with a cluster of strength about 3 MeV higher in good agreement with theory [22], while the proton response might resemble the situation in ^{24}Mg , where much more fragmentation is seen than is predicted by theory. The latter situation can be attributed to $1p \rightarrow sd$ transitions excluded by our truncation of the $1\hbar\omega$ basis, as indicated by a test calculation done for ^{20}Ne [37].

Discussion of stretched transitions in $N \neq Z$ nuclei is complicated by the nonzero ground-state isospin. Because we have a $T = 1$ ground state in ^{26}Mg , an isovector transition can connect to $T = 0$, $T = 1$, or $T = 2$ states depending on the change in T_z in the reaction. Further, the value of Z_{1,T_z} is related to that for the other values of T_z by a Clebsch-Gordan coefficient ratio [31] that, unlike the situation when $T_{\text{g.s.}} = 0$, is not typically unity. It is most convenient to use a diagram to present the relationships between the Z coefficients for different reactions, and it will also prove advantageous to use the same diagram to show the magnitude of Z_{1,T_z}^2 expected from the simplest model for these stretched transitions. Figure 1 shows the value of Z^2 for the possible stretched transitions built on a simple shell-model ground state, the so-called extreme single particle-hole model (ESPHM). Although this nomenclature is technically incorrect (extremely simple might be a better choice of words), we will use ESPHM to denote results from the naive shell model for consistency with the notation of other authors. The absolute magnitude of the rate depends on the $d_{5/2}$ occupancy for pure states built on $T_<$ ($T = 1/2$) and $T_>$ ($T = 3/2$) configurations coupled to an $f_{7/2}$ particle. We use a double line for the $T = 1$ level in the figure as a mnemonic to indicate that it has both $T_<$ and $T_>$ parentage.

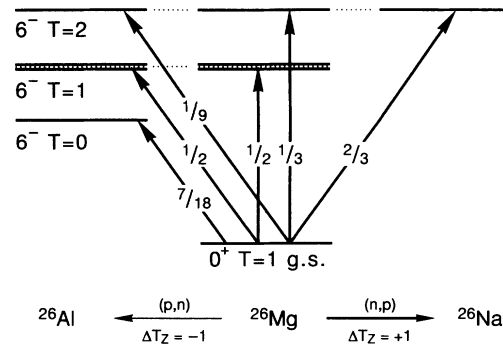


FIG. 1. Schematic diagram showing the isovector transitions for $A = 26$ nuclei considered in this work and the ESPHM estimate of the transition strength for each. The double line for the $T = 1$ level is intended to denote the presence of both $T_<$ and $T_>$ parentage.

There is a wide variety of data, from many different kinds of experiments, available for the stretched 6^- states in ^{26}Mg . Electron scattering data taken by Plum [38] have been analyzed [39] to provide accurate information on those transitions that are predominantly isovector in character. Additional information on isovector transitions is available from the study of the (p, n) reaction at 135 MeV [40], which is the only source of information concerning the $T = 0$ states in ^{26}Al . Unfortunately, the authors of Ref. [40] quote a ratio of their fitted value of $Z_{1,-1}^2$ to an ESPHM value that is only applicable when both the neutron and proton $d_{5/2}$ levels are fully occupied; their tabulated numbers must be converted back to $Z_{1,-1}^2$ before they can be compared to calculations or other data.

Data for the (p, p') reaction [24], when analyzed in conjunction with the electron-scattering data, provide information about the isoscalar response and thus the proton-neutron structure of a transition. Pion scattering data, such as the very limited set in Ref. [41] or the rather complete set of Ref. [42], have the virtue of providing an independent measure of the proton-neutron composition of those transitions where cross sections were measured for both π^+ and π^- .

Calculations were done as described in the previous section. The number of iterations required was different for each isospin T because of differences in the size of the basis space and in the complexity of the spectrum. In particular, many more iterations are required when there are a number of observable fragments that we wish to isolate. A total of 35 iterations were made for the $T = 0$ states, 56 for the $T = 1$ states, and 26 for the $T = 2$ states. Separate calculations were made for the proton and neutron response for $T = 1$ states in addition to those made for the isoscalar and isovector response.

Tables I and II show the lowest converged states in this calculation and compare their properties with the results of several inelastic-scattering experiments. Of particular note is that we get approximately the correct total strength (0.16 versus 0.17 ± 0.02) for the $T = 0$ strength localized near $E_x = 7$ MeV, as shown in Table I and the graphs described below. The predicted strength for

TABLE I. Results for a few of the lowest isovector $M6$ transitions in $A = 26$ nuclei. The first two columns give the theoretical predictions from this work, which are compared to data shown in the remaining columns. Typical experimental uncertainties for Z^2 are in the 15–20 % range. The theoretical excitation energies E_{th} are all measured relative to the ground state of ^{26}Mg .

$T = 0$ states		(p, n) data ^a			
$E_{\text{th}}(\text{MeV})$	$Z_{1,-1}^2$	$E_x(^{26}\text{Al})$	$Z_{1,-1}^2$		
6.82	0.147	6.9	0.123		
7.42	0.017	7.5	0.047		
8.50	0.001	...			
$T = 2$ states		(e, e') data ^b		(p, n) data ^c	
$E_{\text{th}}(\text{MeV})$	$Z_{1,0}^2$	$E_x(^{26}\text{Mg})$	$Z_{1,0}^2$	$E_x(^{26}\text{Al})$	$Z_{1,0}^2$
18.84	0.200	18.0	0.146	18.2	0.135
21.05	0.002	

^aReference [40].

^bReference [39].

^cReference [40] with $Z_{1,-1}^2$ converted to $Z_{1,0}^2$ by applying the isospin Clebsch factor of 3.

$T = 2$ states is about 30% too large and too high in excitation by almost 1 MeV, but the calculation does place the strength mainly in a single observable state (consistent with experiment) as we will see when we look at the spectra below. The lowest $T = 1$ state (see Table II) is predicted to be a neutron state, in agreement with the pion analysis [41, 42] but in disagreement with the proton analysis [24]. The isoscalar strength in the $T = 1$ states above 12 MeV excitation is badly overestimated based on comparison to the pion data (but not the proton data as will be clear below), a feature that can be discussed more easily in terms of the spectra.

Figure 2 shows the isovector $M6$ response in comparison to data from the (p, n) and (e, e') experiments. The shaded histogram represents strengths deduced from the (p, n) reaction [40], displayed as described near the end of Sec. II. (The height of the histogram bar can be compared to the peak of the theory curve and the shaded area of the bar can be compared to the area under the

theoretical curve.) Note that the isovector strength in the 9.3 MeV peak has been divided between $T = 1$ and $T = 0$ states in the proportion described in Ref. [40]. The solid “data points” represent strengths deduced from electron scattering [38] (as fit in Ref. [39]) in the analysis of pion scattering data [42], while the open circles denote the strength deduced from the analysis of these same electron data in conjunction with proton scattering data [24]. (These points, displayed as described in Sec. II, should be compared to the top of the peak in the theoretical spectrum or the top of the histogram bars.) The strength deduced for the $T = 2$ states from the (e, e') data has been converted from $Z_{1,0}^2$ to $Z_{1,-1}^2$ for display in Fig. 2 to facilitate comparison to the (p, n) data.

The isovector response shown in Fig. 2 agrees rather well with the theoretical prediction for $T = 0$ and $T = 2$ states. Specifically, the strength in $T = 0$ states is concentrated near 7 MeV excitation with the total strength predicted in the lowest two states rather close to that measured in the (p, n) experiment, although the distribution of strength between these two states is not correct. Both theory and experiment get a single $T = 2$ state, with the amount of strength and the excitation energy somewhat overpredicted by theory as noted above. The isovector response for the $T = 1$ states shows some qualitative differences between theory and experiment. The strength in the yrast state is overpredicted by about a factor of 2, and the strength in the cluster about 3–7 MeV higher appears to be spread more broadly than predicted. There are some disagreements between the electron scattering and (p, n) data in this higher excitation region (where the charge exchange experiment could have misassigned some $T = 0$ states as $T = 1$ states), but none that would alter our overall conclusions that this calculation still underestimates the fragmentation in $T = 1$ states.

Figure 3 shows the isoscalar $M6$ response for $T = 1$ states in the upper panel. The isoscalar response should be compared to the isovector response already displayed in the middle panel of Fig. 2; the experimental results from pion data (solid points) [42] and proton data (open circles) [24] are shown in the same way in both figures. (It happens that $Z_{1,0}^2 = Z_{1,-1}^2$ for $T = 1$ states, so it is correct to compare directly the isoscalar strength with

TABLE II. Results for low-lying 6^- $T = 1$ states in ^{26}Mg . Theoretical predictions from this work are given in the first three columns and compared to the data for corresponding levels in the remaining columns. Typical experimental uncertainties in Z are ± 0.01 with larger (up to ± 0.03) errors in some Z_0 values.

$E_{\text{th}}(\text{MeV})$	$T = 1$ states		Pion and electron data ^a			(p, n) data ^b	
	Z_0	Z_1	$E_x(^{26}\text{Mg})$	Z_0	Z_1	$E_x(^{26}\text{Al})$	Z_1
9.94	0.260	0.311	9.2	0.15	0.21	9.3	0.200
11.64	0.011	0.046	12.0	-0.16	0.00	...	
12.20	0.110	0.070	12.5	0.06	0.22	12.5	0.201
...			12.9	-0.13	0.11	...	
13.10	0.356	-0.078	13.0	0.03	0.11	13.1	0.161

^aReference [42] harmonic-oscillator analysis.

^bReference [40] results converted to $T_x = 0$.

$T_z = 0$ in Fig. 3 to the isovector strength with $T_z = -1$ in Fig. 2.) Note the concentration of isoscalar strength predicted near 13 MeV excitation, which is not seen in the pion results [42] but is seen in the proton scattering analysis [24]. This proton analysis gives $Z_0^2 \approx 0.12$ compared to the prediction of 0.13 in the region near 13 MeV. Since the proton data give the wrong answer for the neutron-proton composition of the lowest $T = 1$ state, it is difficult to know how much weight to give to this last result. We note in passing that there is an alternate fit in Ref. [24] that does give the lowest $T = 1$ state a neutron character, albeit not a very good one, and these authors discuss concerns about the relative phase of the isoscalar and isovector parts of the NN interaction. It is important that the source of this disagreement between proton and pion analyses be identified so that an accurate isoscalar spectrum can be obtained from data for $N \neq Z$

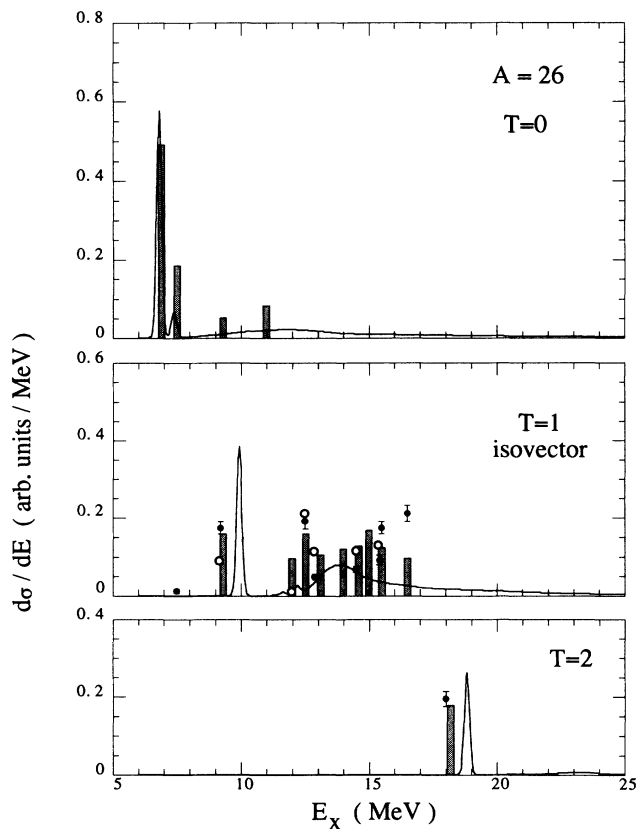


FIG. 2. Isovector $M6$ response functions in $A = 26$ nuclei for $T = 0$ (top), 1 (middle), and 2 (bottom) transitions from this work are shown with a solid curve. In all cases the strength is for $\Delta T_z = -1$. The shaded histograms denote the (p, n) strength [40] while the solid data points show the strength deduced from electron data [39] with some minor (about 10%) corrections from the pion data [42]. The open circles for the $T = 1$ states are data points for the isovector strength deduced from the analysis of proton scattering data [24]. As discussed in Sec. II, the data points should be compared to the peak of the strength-function curve and the top of the histogram bar; the shaded area of the histogram bar also can be compared to the area under the strength-function curve.

nuclei. Several ongoing studies are looking closely at the properties of the isoscalar tensor NN interaction, which is dominated by exchange and has not been tested as extensively as the direct-dominated isovector tensor NN interaction [43].

Figure 3 shows the neutron-proton decomposition of the response for the $T = 1$ states in the lower two panels. Here the theory is compared to a histogram showing the strengths deduced from analysis of recent pion data [42]. The distribution from the analysis of proton data is not shown because that work gives the suspect result that the lowest state is a proton excitation. Notice that the neutron response shows much strength in the yrast state as expected, although this strength is overestimated and the neutron strength in the cluster about 4 MeV higher is correspondingly underestimated. The proton response is much weaker and more widely fragmented than we predict.

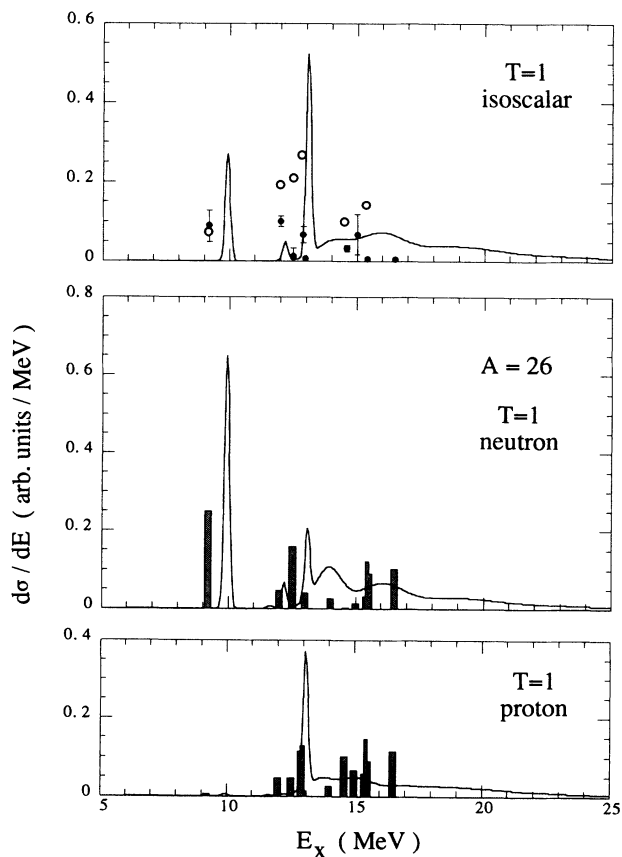


FIG. 3. Additional $M6$ response functions (all with $\Delta T_z = 0$) for $T = 1$ states in ^{26}Mg . The top panel shows the isoscalar strength from this calculation (solid curve) compared to solid data points that denote the result of an analysis of pion scattering data [42] and open circles that denote the result of the proton scattering analysis [24]. The lower two panels show the neutron and proton decomposition of the strength distributions compared to a histogram that denotes the result of the pion analysis of Ref. [42]. The curves and histograms in the lower two panels contain the same information as the curves and solid data points in the top panel of this figure and the middle panel of Fig. 2.

These results represent quite an improvement over those of Amusa and Lawson reported in Ref. [24] for the $T = 1$ states in ^{26}Mg . The easiest comparison we can make is for the lowest state, where they obtained $Z_1 = 0.39$ and $Z_0 = 0.30$. The larger basis used for this study gives 0.31 and 0.26 for these amplitudes, which are to be compared to experimental values of 0.20 and 0.15, respectively. The improvement in the isovector strength has eliminated more than half of the discrepancy between theory and experiment. Further, unlike Ref. [24], we do not see an observable $T = 2$ state a few MeV above the known level.

Another way to look at these results, one that emphasizes the fraction of the ESPHM strength expected in a certain region of E_x , is to examine integrals of the $M6$ strength distribution. Figure 4 shows the sequence of partial sums of the strength in each part of the response; that is, we plot

$$\sum_{E=0}^{E_x} Z^2(E)$$

as a function of E_x . Table III gives the relevant total sums and compares them to the integrated experimental strength as well as the integral of the theoretical strength over roughly the range of excitation where the data exist. As Fig. 4 makes clear, there can be as much as 25% of the strength shifted to high excitation where it is not seen by experiment. It is important that experimental values for the integrated strength be compared to a similar integral of the theoretical response and not just to Σ or the ESPHM value.

The results shown in Fig. 4 demonstrate that we have excellent agreement between this theoretical calculation and the (p, n) data for the $T = 0$ and $T = 1$ states up to the maximum E_x probed by the experiment. The theory is too high for the lowest state and too low for the next states, another indication that all features of the fragmentation are not described in detail, but the total strength in this region is correct. Further, the results for

TABLE III. Integrals of $M6$ strength for $A = 26$. The theory entries give the total sum (Σ is the value for the basis truncation used in this work) as well as the integral over the specified region of excitation energy. Typical uncertainties in the integrated experimental strength are about 15%.

\int theory	Isovector			Isoscalar
	$T = 0$	$T = 1$	$T = 2$	$T = 1$
ESPHM ^a	0.389	0.500	0.333	0.833
Σ	0.313	0.402	0.267	0.668
This work	0.229 ^b	0.320 ^c	0.200 ^d	0.440 ^e

\int data	Isovector			Isoscalar
	$T = 0$	$T = 1$	$T = 2$	$T = 1$
(e, e') Ref. [39]		0.267	0.146	
(p, n) Ref. [40]	0.205	0.290	0.135	
(p, p') Ref. [24]		0.167	0.122	0.250
(π, π') Ref. [42]		0.270	0.144	0.095

^aNaive shell-model result.

^bIntegral of Z_{1,T_z}^2 for $T_z = -1$ up to 12 MeV excitation; value is 0.28 if integrated to 17 MeV excitation.

^cIntegral of Z_{1,T_z}^2 for $T_z = 0$ up to 17 MeV excitation; note that $T_z = -1$ integral is the same number.

^dIntegral of Z_{1,T_z}^2 for $T_z = 0$ up to 20 MeV excitation; note that $T_z = -1$ integral is a factor of 3 smaller.

^eIntegral of $Z_{0,0}^2$ up to 17 MeV excitation.

the isovector strength in $T = 1$ states from the proton analysis, which are essentially the same as the pion analysis because both are dominated by the electron-scattering data, also agree on average with the integrated (p, n) data in the region where both exist. The $T = 2$ integral is not very informative because only one state is seen.

The integrated strength for $T = 1$ states in the region $E_x < 17$ MeV obtained by Amusa and Lawson [24] does not show nearly the same level of agreement. Their isovector strength gives 0.39, in comparison to the result of 0.32 from this study and the experimental value of about 0.28. Their isoscalar strength gives an integral

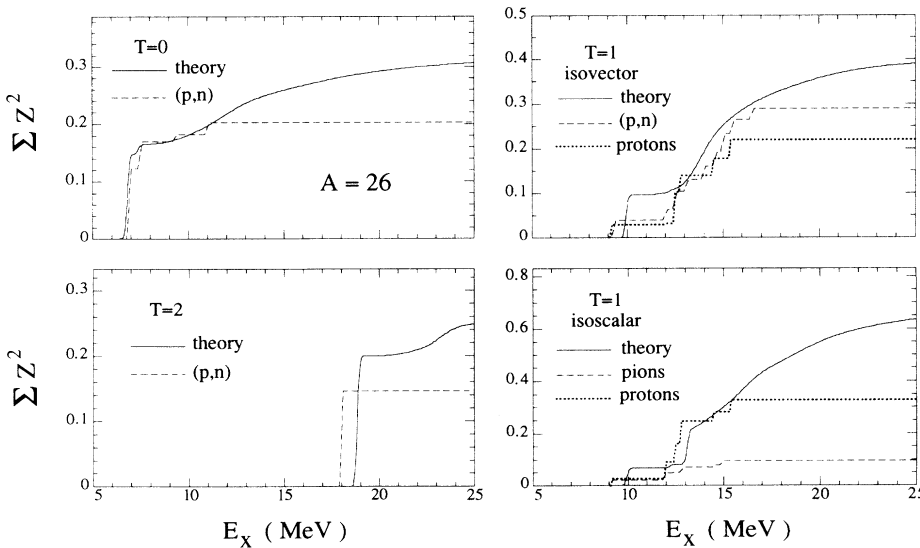


FIG. 4. $M6$ strength for $A = 26$ nuclei integrated up to a given E_x . The solid curve shows the theoretical prediction, the dashed curve shows the (p, n) [40] and pion [42] results for isovector and isoscalar transitions, respectively, and the dotted curve shows the results from the proton analysis [24] for $T = 1$ states. The maximum in each panel is the ESPHM “sum rule” to emphasize the fraction of the sum exhausted over a given energy region.

of 0.56, in comparison to the present result of 0.44 and an experimental value that falls somewhere in the range from 0.10 to 0.25. The important conclusion we reach is that this larger basis is sufficient to describe the fragmentation of isovector strength but inadequate to explain the isoscalar fragmentation.

As already noted above, the big disagreement between the results of the pion [42] and proton [24] analyses concerns the isoscalar strength. The problem is quite clear in the lower right panel of Fig. 4. It is interesting that the proton results agree rather well with the theoretical prediction. The proton analysis gives the wrong relative phase between isoscalar and isovector, misidentifying the lowest state as a proton excitation, so there must be doubts about this analysis. However, the proton experiment clearly does see more scattering strength around 12–13 MeV excitation, so a simple phase problem with the NN interaction may not explain this discrepancy. It is important that the source of this problem, which is seen for other nuclei as well, be identified and corrected. In addition, there is a significant conflict concerning the isovector strength at $E_x = 12.0$ and 15.0 MeV between the (p, n) data [40] and the electron scattering analysis [39] that affects our conclusions and needs resolution. There is an unanalyzed peak near 15.0 MeV in the proton scattering spectrum [24] that could have a bearing on this matter. Further, there are as-yet-unpublished claims based on high resolution electron scattering [44] that some transitions reported in these published papers are incorrectly identified or contaminated by lower multiple transitions.

We can summarize the theoretical results for both isospin transfers as follows: about 20% of the strength is lost because of depletion of the $d_{5/2}$ orbit ($\Sigma = 0.668$ instead of 0.833) in the ground state; another 20–25% cannot be seen because it is scattered at high excitation, beyond the range explored in the experiments. The theoretical prediction for the *isovector* strength is about 20% above the experimental result in the same region of excitation energy, but some of the difference between theory and experiment is no doubt due to small unobservable fragments that are included in our integrated strength. The calculation does not have sufficient detail to identify which parts of the response might be too weak to see in these experiments. Theory predicts more than four times more *isoscalar* strength than is seen in the pion experiment, but is only about 75% above that claimed in the proton scattering experiment. We do expect fragmentation of isoscalar strength to be underestimated by our calculations based on earlier results [22], but the difference between these two experiments is large and must be resolved to clarify this situation. Nonetheless, theory does predict larger fragmentation effects for the isoscalar transitions, albeit not large enough to explain the data.

Overall, we get a very clear picture of the fragmentation of the $M6$ strength in ^{26}Mg from the comparison of these calculations to the data. The isovector strength distribution and integrated strength in $T = 0$ and $T = 2$ states is in good agreement with the data. The integrated isovector strength agrees well with the data for $T = 1$ states although its distribution in E_x does not.

The isoscalar strength appears to be much more fragmented than we predict, although this last conclusion should await a resolution of the conflict between the analyses of pion and proton data for these states.

IV. ^{30}Si

The situation in ^{30}Si is that both the neutron and proton $d_{5/2}$ levels are filled and a pair of neutrons occupies the $s_{1/2}$ level. Thus the proton response might be expected to resemble the situation in ^{28}Si , where there is a strong state with a cluster of strength about 3 MeV higher in good agreement with theory [22], while the neutron response might resemble the situation in ^{32}S , where there is much more fragmentation predicted by theory and seen in the experiments because of fragmentation of the $d_{5/2}$ level [20]. The distribution of levels populated by pickup reactions on ^{30}Si support this assertion that the $d_{5/2}$ neutrons are more fragmented than the $d_{5/2}$ protons [36].

As in the previous section, it is convenient to use a diagram to display the magnitude of $Z_{1,T}^2$ expected from the simplest model for these stretched transitions and to show the relationships between the Z coefficients for different reactions. Figure 5 shows the value of Z^2 for the possible stretched transitions built on a simple shell-model ground state, the so-called ESPHM. The absolute magnitude of the rate depends on the $d_{5/2}$ occupancy for pure states built on $T_<$ and $T_>$ configurations coupled to an $f_{7/2}$ particle. We use a double line for the $T = 1$ level in the figure as a mnemonic to indicate that it has both $T_<$ and $T_>$ parentage.

The only published data available for the 6^- states in ^{30}Si are the excitation energies obtained from the $^{27}\text{Al}(\alpha, p\gamma)^{30}\text{Si}$ reaction [45]. Experiments, as yet unpublished, also have been performed with electron scattering [46] and the (p, n) reaction [47].

Calculations were done as described in Sec. II. Once again the number of iterations made for each isospin T varied depending on the number of observable fragments that had to be isolated. A total of 26 iterations were made for the $T = 0$ states, 56 for the $T = 1$ states,

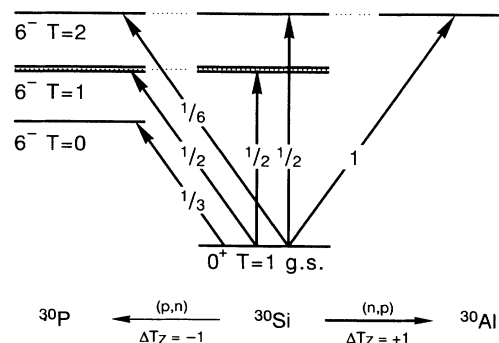


FIG. 5. Schematic diagram showing the isovector transitions for $A = 30$ nuclei considered in this study and the ESPHM estimate of the transition strength for each. The double line for the $T = 1$ level is intended to denote the presence of both $T_<$ and $T_>$ parentage.

TABLE IV. Theoretical results for a few of the lowest 6^- states in $A = 30$ nuclei. The excitation energies E_{th} are all measured relative to the ground state of ^{30}Si .

$T = 0$ states		$T = 1$ states			$T = 2$ states	
E_{th} (MeV)	$Z_{1,-1}^2$	E_{th} (MeV)	Z_0	Z_1	E_{th} (MeV)	$Z_{1,0}^2$
5.8	0.038	8.7	0.157	0.142	16.2	0.185
6.7	0.089	8.8	0.179	0.191	17.8	0.052
8.0	0.038	

and 36 for the $T = 2$ states. The proton and neutron response was calculated for $T = 1$ states in addition to the isoscalar and isovector response.

Table IV shows the spectroscopic amplitudes for the lowest converged states in this calculation. Figure 6 shows the isovector $M6$ response for $T = 0, 1$, and 2 states, which is essentially the spectrum predicted for the (p, n) or (e, e') reactions. (All excitation energies are relative to the ground state of ^{30}Si .) Of particular note is the prediction that the lowest $T = 0$ and $T = 1$ states will not be the strongest, and the suggestion that a second $T = 2$ state might be observable about 2 MeV above the yrast state.

The $6^-, T = 1$ states from this calculation are in reasonable agreement with those seen in the $(\alpha, p\gamma)$ reaction [45]. The lowest state, at 9.1 MeV, matches up with the doublet we predict at 8.7 and 8.8 MeV. We do not have any state near 9.8 MeV, which is identified with a $K = 3^-$ band. This is plausible because this calculation would not be expected to describe a predominantly collective state, which might not carry any $M6$ strength

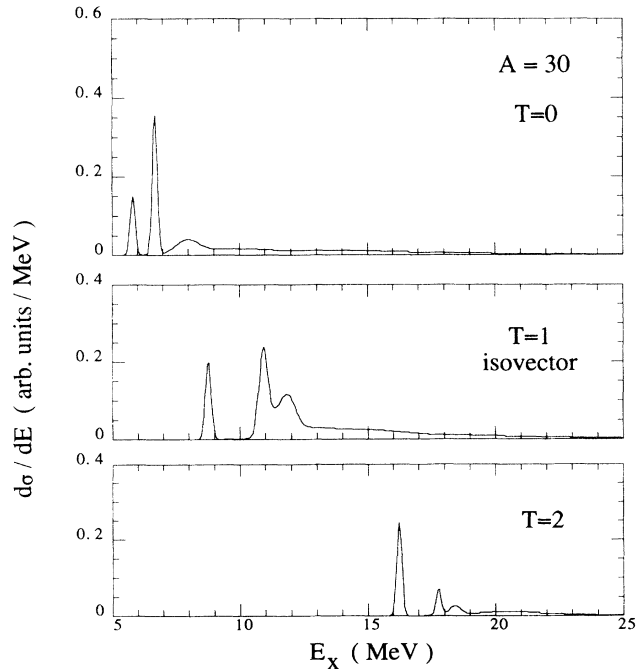


FIG. 6. Isovector $M6$ response functions in $A = 30$ nuclei for $T = 0$ (top), 1 (middle), and 2 (bottom) transitions from this calculation are shown with a solid curve. In all cases the strength is for $\Delta T_z = -1$.

unless mixing with a rotational state splits the doublet predicted at lower E_x . The states seen at 10.6 and 11.5 MeV can be identified with several states that are predicted around 11 MeV.

Preliminary results from the (p, n) reaction [47] are also encouraging. Agreement with the spectrum of $T = 0$ states appears to be excellent, but the $T = 2$ strength is overestimated by a factor of 2. The situation for $T = 1$ states is less clear because the (p, n) [47] and electron-scattering [46] experiments do not see all of the same states. Any detailed conclusions must await publication of the final results of both experiments, and for this reason no data are shown in the figure.

Figure 7 shows the isoscalar $M6$ spectrum for $T = 1$ states as well as the proton-neutron decomposition of the response. The latter is important when considering pion-

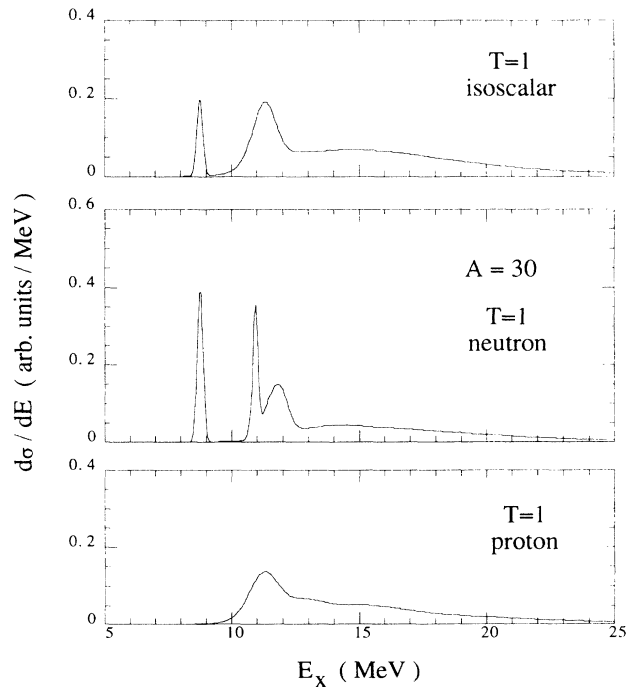


FIG. 7. Additional $M6$ response functions (all with $\Delta T_z = 0$) for $T = 1$ states in ^{30}Si . The top panel shows the isoscalar strength from this study while the lower two panels show the neutron and proton decomposition of the strength distribution. The curves in the lower two panels contain the same information as the curves in the top panel of this figure and the middle panel of Fig. 6.

TABLE V. Integrals of $M6$ strength for $A = 30$. The theory entries give the total sum (Σ is the value for the basis used in this work) as well as the integral over the specified region of excitation energy.

\int theory	Isovector			Isoscalar
	$T = 0$	$T = 1$	$T = 2$	$T = 1$
ESPHM ^a	0.333	0.500	0.500	1.000
Σ	0.312	0.452	0.420	0.873
This work	0.197 ^b	0.364 ^c	0.319 ^d	0.516 ^e

^aNaive shell-model result.

^bIntegral of Z_{1,T_z}^2 for $T_z = -1$ up to 10 MeV excitation; value is 0.26 if integrated to 15 MeV excitation.

^cIntegral of Z_{1,T_z}^2 for $T_z = 0$ up to 15 MeV excitation; note that $T_z = -1$ integral is the same number.

^dIntegral of Z_{1,T_z}^2 for $T_z = 0$ up to 20 MeV excitation; note that $T_z = -1$ integral is a factor of 3 smaller.

^eIntegral of $Z_{0,0}^2$ up to 15 MeV excitation.

scattering experiments. It is clear that the lowest $T = 1$ state is again predicted to be a neutron excitation, but that it will not carry as much strength as the comparable level in ^{26}Mg , Fig. 3. More strength has been moved to higher excitation and the neutron strength is broken into large, observable pieces. The proton strength is clustered in the region about 2–3 MeV above the lowest $T = 1$ state.

The distribution of strength in various regions of excitation can also be seen in Fig. 8, where running integrals of the strength distribution are shown. Again we set the maximum value in each panel at the ESPHM value. Table V gives the total sums and corresponding integrals over the region of excitation covered by the experiments. On average, about 60% of the ESPHM strength is predicted to be observable by these experiments, with important contributions coming from a broad distribution of weak states.

V. SUMMARY

The particular emphasis in this paper has been on the information that can be obtained by examining the isospin structure of “stretched” strength in $N \neq Z$ nuclei. A variety of one-step reactions can be used to identify the fragmentation of the unique stretched configuration amongst the many 6^- states. In $N \neq Z$ nuclei, mixing between proton and neutron configurations provides a way to increase the visibility of the elusive isoscalar $M6$ strength distribution.

We see that the main features of the reduction and redistribution of $M6$ strength in ^{26}Mg can be described well by large-basis shell-model calculations: the loss of $M6$ strength results from fragmentation of the “stretched” configuration by conventional configuration mixing. In particular, the results for isovector transitions are quite good. The spectra for $T = 0$ and $T = 2$ states are described rather well and the integrated strength for $T = 1$ states is in very good agreement with theory over the range studied experimentally. The model shows greater fragmentation of isoscalar strength than isovector strength, the key result (emphasized in Ref. [3]) that cannot be obtained in core-polarization models, but significantly underestimates the isoscalar fragmentation. There is substantial uncertainty about this last conclusion because the integrated isoscalar strength does agree well with that extracted from proton scattering data [24] but the reliability of this analysis is uncertain.

The key ingredients in these calculations appear to be the use of a basis with sufficiently many degrees of freedom and an effective Hamiltonian that gives a reasonably correct description of ground-state correlations in the sd shell. Both are important because it is the admixture of other 6^- configurations by mixing within the sd shell that has fragmented the “stretched” configuration. We emphasize that it is the full spectrum of the $M6$ response that provides the most stringent test of any model.

Predictions are made for ^{30}Si . The $M6$ response for

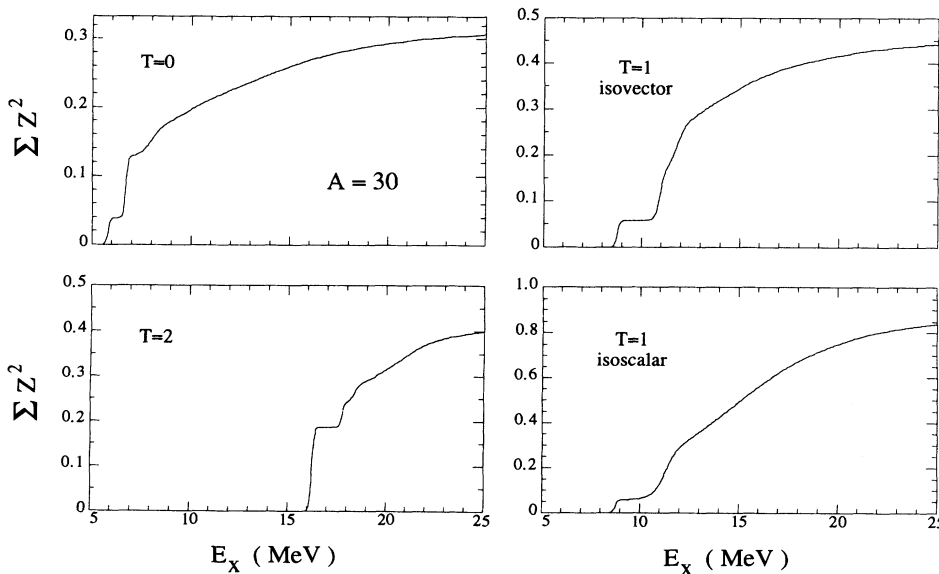


FIG. 8. $M6$ strength for $A = 30$ nuclei integrated up to a given E_x . The curve shows the theoretical prediction from this work. The maximum in each panel is the ESPHM “sum rule” to emphasize the fraction of the sum exhausted over a given energy region.

$A = 30$ nuclei should have similar features to that seen in $A = 26$, with the model predicting that the number of large, observable fragments should increase. A detailed comparison of the results of the (p, n) experiment done on this target [47] with the predictions from the present study should be most interesting.

The most important theoretical and/or experimental issue is the resolution of the large disagreement between the proton and pion analyses concerning the neutron-proton or isovector-isoscalar composition of $T = 1$ states in $N \neq Z$ nuclei. There are a number of other theoretical issues. The most important of these is that the failure to use a full $1\hbar\omega$ basis omits p and fp configurations that become important away from the middle of the shell and make it impossible to remove spurious center-of-mass effects from the calculation. The latter are only a few % effect in the strong transitions examined here, but it would be better if they were not present. The crude choice of Hamiltonian, made so that these results

will be consistent with the other calculations made for the $M6$ response in sd -shell nuclei, also leaves room for improvement. Finally, most of the states discussed here are unbound, and continuum effects can produce significant changes in the distribution of proton and neutron strength [48].

ACKNOWLEDGMENTS

Special thanks to Ben Clausen and Luis Garcia for allowing us timely access to their data, and to John Philpott, John Millener, Alex Brown, and Atsushi Yokoyama for informative discussions. This work was supported in part by DOE Contract No. DE-FG05-92ER40750, and the Florida State University Supercomputer Computations Research Institute, which is partially funded by the U.S. Department of Energy through Contract No. DE-FC05-85ER250000.

-
- [1] P.J. Moffa and G.E. Walker, Nucl. Phys. **A222**, 140 (1974).
 - [2] R.A. Lindgren, W.J. Gerace, A.D. Bacher, W.G. Love, and F. Petrovich, Phys. Rev. Lett. **42**, 1524 (1979).
 - [3] F. Petrovich, W.G. Love, A. Picklesimer, G.E. Walker, and E. Siciliano, Phys. Lett. **95B**, 166 (1980).
 - [4] F. Petrovich and W.G. Love, Nucl. Phys. **A354**, 499c (1981).
 - [5] F. Petrovich, J.A. Carr, and H. McManus, Annu. Rev. Nucl. Part. Sci. **36**, 29 (1986).
 - [6] R.A. Lindgren, M. Leuschner, B.L. Clausen, R.J. Peterson, M.A. Plum, and F. Petrovich, Can. J. Phys. **65**, 666 (1987).
 - [7] T. Suzuki, S. Krewald, and J. Speth, Phys. Lett. **107B**, 9 (1981).
 - [8] F. Osterfeld, S. Krewald, J. Speth, and T. Suzuki, Phys. Rev. Lett. **49**, 11 (1982).
 - [9] P. Blunden, B. Castel, and H. Toki, Nucl. Phys. **A440**, 647 (1985).
 - [10] S. Krewald and J. Speth, Phys. Rev. Lett. **45**, 417 (1980).
 - [11] I. Hamamoto, J. Lichtenstadt, and G. F. Bertsch, Phys. Lett. **93B**, 213 (1980).
 - [12] J. Speth, V. Klemt, J. Wambach, and G.E. Brown, Nucl. Phys. **A343**, 382 (1980).
 - [13] P. Blunden, B. Castel, and H. Toki, Z. Phys. A **312**, 247 (1983).
 - [14] A. Yokoyama and H. Horie, Phys. Rev. C **36**, 1657 (1987).
 - [15] K. Muto, Phys. Lett. B **213**, 115 (1988).
 - [16] D.J. Millener and D. Kurath, Nucl. Phys. **A255**, 315 (1975).
 - [17] A. Amusa and R.D. Lawson, Phys. Rev. Lett. **51**, 103 (1983).
 - [18] A.G.M. van Hees and P.W.M. Glaudemans, Z. Phys. A **314**, 323 (1983); **315**, 223 (1984).
 - [19] J.A. Carr, S.D. Bloom, F. Petrovich, and R.J. Philpott, Phys. Rev. Lett. **62**, 2249 (1989); **63**, 918(E) (1989).
 - [20] B.L. Clausen *et al.*, Phys. Rev. Lett. **65**, 547 (1990).
 - [21] N. Tamimi *et al.*, Phys. Rev. C **45**, 1005 (1992).
 - [22] J.A. Carr, S.D. Bloom, F. Petrovich, and R.J. Philpott, Phys. Rev. C **45**, 1145 (1992).
 - [23] D.B. Holtkamp, S.J. Seestrom-Morris, D. Dehnhard, H.W. Baer, C.L. Morris, S.J. Greene, C.J. Harvey, D. Kurath, and J.A. Carr, Phys. Rev. C **31**, 957 (1985); **41**, 1319(E) (1990).
 - [24] R.E. Segel *et al.*, Phys. Rev. C **39**, 749 (1989).
 - [25] D.J. Millener, Phys. Rev. C **36**, 1643 (1987).
 - [26] D.M. Manley *et al.*, Phys. Rev. C **34**, 1214 (1986).
 - [27] R.A. Lindgren, J.B. Flanz, R.S. Hicks, B. Parker, G.A. Peterson, R.D. Lawson, W. Teeters, C.F. Williamson, S. Kowalski, and X.K. Maruyama, Phys. Rev. Lett. **46**, 706 (1981).
 - [28] B.D. Anderson *et al.*, Phys. Rev. C **46**, 504 (1992).
 - [29] B.H. Wildenthal, Prog. Part. Nucl. Phys. **11**, 5 (1984).
 - [30] J.P. Schiffer and W.W. True, Rev. Mod. Phys. **48**, 191 (1976).
 - [31] See Appendix A.1 in F. Petrovich, R.H. Howell, C.H. Poppe, S.M. Austin, and G.M. Crawley, Nucl. Phys. **A383**, 355 (1982).
 - [32] R.R. Whitehead, Nucl. Phys. **A182**, 290 (1972).
 - [33] S.D. Bloom, Prog. Part. Nucl. Phys. **11**, 505 (1984).
 - [34] R.R. Whitehead, in *Moment Methods in Many Fermion Systems*, edited by B.J. Dalton, S.M. Grimes, J.P. Vary, and S.A. Williams (Plenum, New York, 1979), p. 235; Bull. Am. Phys. Soc. **32**, 1012 (1987).
 - [35] R.F. Hausman, Ph.D. thesis, LLNL Report No. UCRL-52178, 1976.
 - [36] P.M. Endt and C. van der Leun, Nucl. Phys. **A521**, 1 (1990).
 - [37] E.K. Warburton and B.A. Brown, Phys. Rev. C **46**, 923 (1992).
 - [38] M.A. Plum, Ph.D. thesis, University of Massachusetts, 1985.
 - [39] B.L. Clausen, R.J. Peterson, and R.A. Lindgren, Phys. Rev. C **38**, 589 (1988).
 - [40] C. Lebo, B.D. Anderson, T. Chittrakarn, A.R. Baldwin, R. Madey, J.W. Watson, and C.C. Foster, Phys. Rev. C **38**, 1099 (1988).

- [41] R.A. Lindgren *et al.*, Phys. Rev. C **44**, 2413 (1991).
- [42] B.L. Clausen, R.J. Peterson, C. Kormanyos, J.E. Wise, A.B. Kurepin, and Yu.K. Gavrilov, Phys. Rev. C **48**, 1632 (1993).
- [43] S. Chang *et al.*, Bull. Am. Phys. Soc. **38**, 1830 (1993); K. Cromer *et al.*, *ibid.* **38**, 1847 (1993).
- [44] K.K. Seth, private communication.
- [45] E. Bitterwolf, P. Betz, A. Burkard, F. Glatz, F. Heindinger, Th. Kern, R. Lehmann, S. Norbert, J. Siefert, and H. Röpke, Z. Phys. A **298**, 279 (1980).
- [46] L. Knox, R.A. Lindgren, B.L. Clausen, B. Berman, D. Zubanov, M. Farkhondeh, L.W. Fagg, and M. Manley, Bull. Am. Phys. Soc. **34**, 1812 (1989); B.L. Clausen and R.A. Lindgren, private communication.
- [47] L. Garcia, Ph.D. thesis, Kent State University, 1992; L. Garcia and B.D. Anderson, private communication.
- [48] D. Halderson, R.J. Philpott, J.A. Carr, and F. Petrovich, Phys. Rev. C **24**, 1095 (1981).

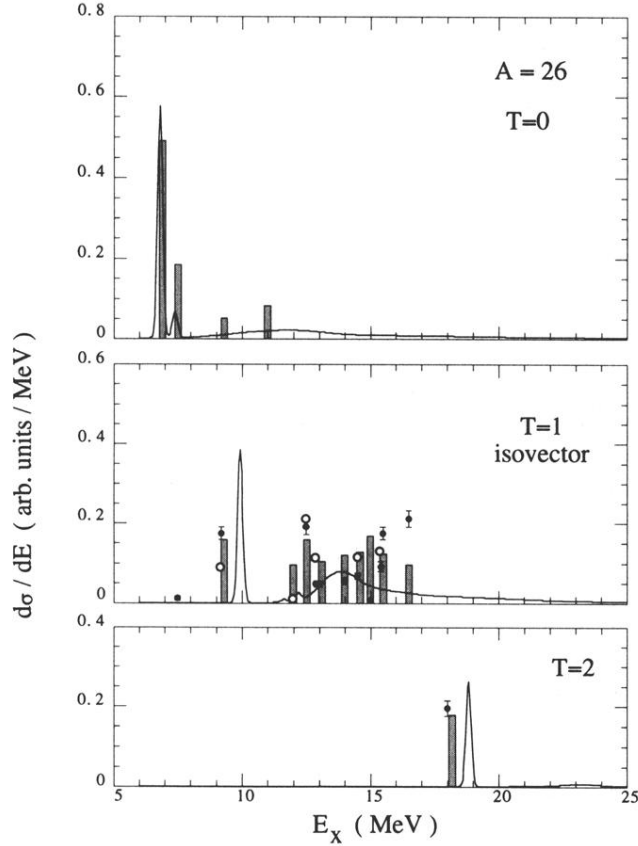


FIG. 2. Isovector $M6$ response functions in $A = 26$ nuclei for $T = 0$ (top), 1 (middle), and 2 (bottom) transitions from this work are shown with a solid curve. In all cases the strength is for $\Delta T_z = -1$. The shaded histograms denote the (p, n) strength [40] while the solid data points show the strength deduced from electron data [39] with some minor (about 10%) corrections from the pion data [42]. The open circles for the $T = 1$ states are data points for the isovector strength deduced from the analysis of proton scattering data [24]. As discussed in Sec. II, the data points should be compared to the peak of the strength-function curve and the top of the histogram bar; the shaded area of the histogram bar also can be compared to the area under the strength-function curve.

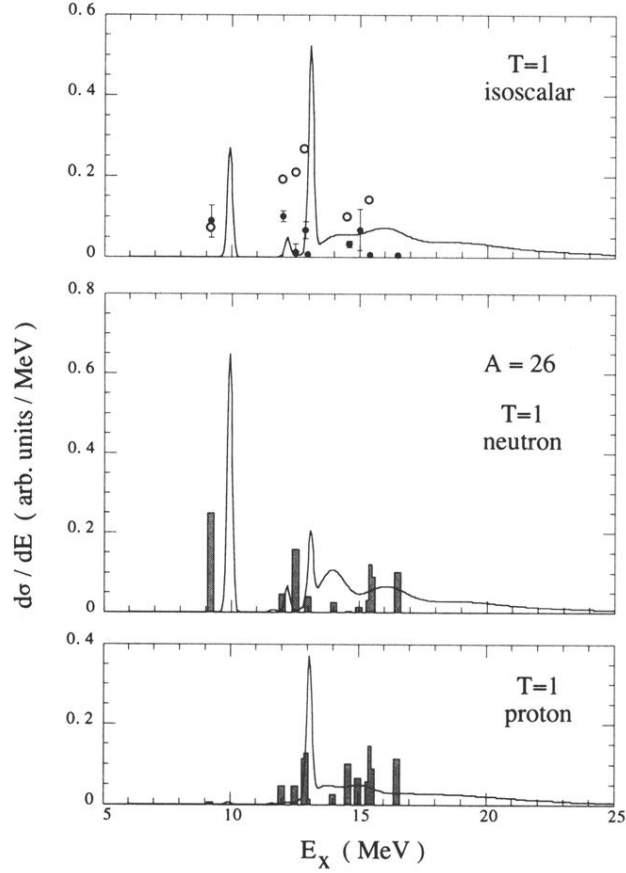


FIG. 3. Additional $M6$ response functions (all with $\Delta T_z = 0$) for $T = 1$ states in ^{26}Mg . The top panel shows the isoscalar strength from this calculation (solid curve) compared to solid data points that denote the result of an analysis of pion scattering data [42] and open circles that denote the result of the proton scattering analysis [24]. The lower two panels show the neutron and proton decomposition of the strength distributions compared to a histogram that denotes the result of the pion analysis of Ref. [42]. The curves and histograms in the lower two panels contain the same information as the curves and solid data points in the top panel of this figure and the middle panel of Fig. 2.